was not observed up to 48 h, this result of the temporary occlusion of the lobe provided an interesting phenomena; however, the lack of temporal portal venous flow could become atrophic if portal venous ischemia had lasted longer. The duration for the "point of no return" should be investigated in further research.

In conclusion, a temporary blood flow obstruction of the portal vein may be a significant trigger for liver regeneration, even with an obstruction of 12 h. The histological changes in the unobstructed lobe and obstructed lobe in cases of temporary blood flow obstruction of the portal vein and at 48 h after reperfusion were described.

COMMENTS

Background

Permanent obstruction of the portal vein, as clinically applied in portal branch ligation (PBL) or percutaneous transhepatic portal venous embolization, evokes liver regeneration. This technique enables relatively major hepatic resection for malignancy in an occluded liver lobe. In addition, PBL has been used to induce a regenerative stimulus for transplanted hepatocytes or pancreatic islet cells for cell therapy.

Research frontiers

Portal venous branch ligation or embolization can induce atrophy of the ligated lobe, while inducing hypertrophy of a non-ligated lobe, which enables extended hepatectomy for a malignant tumor in a ligated lobe. In addition, PBL has been used as a regenerative stimulator to induce transplanted cell proliferation in animal models of hepatocyte based cell therapy. The length of time of occlusion required to induce remnant liver regeneration, *i.e.*, temporary portal venous occlusion, remains unknown.

Innovations and breakthroughs

The histological changes and the status of liver regeneration were compared between a liver biopsy performed on each lobe after temporary obstruction of the portal vein in the same rat liver, and the liver extracted at the time of sacrifice (48 h after reperfusion).

Peer review

This research is very important because it shows that a temporary obstruction of the portal vein as a trigger of liver regeneration. Recently, it has been used as a regenerative stimulator to induce transplanted cell proliferation. Thus, the manuscript approached an interesting subject from the surgical and scientific points of view; however, several aspects should be better evaluated.

REFERENCES

1 **Yu JH**, Zhang WG, Jiang GX, Zhao JY, Li H, Wang ZD, Cui YF. Ischemia/reperfusion in clamped lobes facilitates liver regeneration of non-clamped lobes after selective portal vein ligation. *Dig Dis Sci* 2012; **57**: 3178-3183 [PMID: 22752666 DOI: 10.1007/s10620-012-2298-x]

2 **van Lienden KP**, van den Esschert JW, de Graaf W, Bipat S, Lameris JS, van Gulik TM, van Delden OM. Portal vein embolization before liver resection: a systematic review. *Cardiovasc Intervent Radiol* 2013; **36**: 25-34 [PMID: 22806245 DOI: 10.1007/s00270-012-0440-y]

3 **Rauchfuss F**, Lambeck S, Claus RA, Ullmann J, Schulz T, Weber M, Katenkamp K, Guthke R, Bauer M, Settmacher U. Sustained liver regeneration after portal vein embolization --a human molecular pilot study. *Dig Liver Dis* 2012; **44**: 681-688 [PMID: 22561445 DOI: 10.1016/j.dld.2012.04.002]

4 **Yang K**, Du C, Cheng Y, Li Y, Gong J, Liu Z. Augmenter of liver regeneration promotes hepatic regeneration depending on the integrity of Kupffer cell in rat small-for-size liver transplantation. *J Surg Res* 2013; **183**: 922-928 [PMID: 23522454 DOI: 10.1016/j.jss.2013.02.033]

5 **Ebata T**, Yokoyama Y, Igami T, Sugawara G, Takahashi Y, Nagino M. Portal vein embolization before extended hepatectomy for biliary cancer: current technique and review of 494 consecutive embolizations. *Dig Surg* 2012; **29**: 23-29 [PMID: 22441616 DOI: 10.1159/000335718]

6 **Imamura H**, Shimada R, Kubota M, Matsuyama Y, Nakayama A, Miyagawa S, Makuuchi M, Kawasaki S. Preoperative portal vein embolization: an audit of 84 patients. *Hepatology* 1999; **29**: 1099-1105 [PMID: 10094953]

7 **Okabe H**, Beppu T, Nakagawa S, Yoshida M, Hayashi H, Masuda T, Imai K, Mima K, Kuroki H, Nitta H, Hashimoto D, Chikamoto A, Ishiko T, Watanabe M, Yamashita Y, Baba H. Percentage of future liver remnant volume before portal vein embolization influences the degree of liver regeneration after hepatectomy. *J Gastrointest Surg* 2013; **17**: 1447-1451 [PMID: 23715651]

8 **Shindoh J**, Vauthey JN, Zimmitti G, Curley SA, Huang SY, Mahvash A, Gupta S, Wallace MJ, Aloia TA. Analysis of the efficacy of portal vein embolization for patients with extensive liver malignancy and very low future liver remnant volume, including a comparison with the associating liver partition with portal vein ligation for staged hepatectomy approach. *J Am Coll Surg* 2013; **217**: 126-133; discussion 133-134 [PMID: 23632095 DOI: 10.1016/j.jamcollsurg.2013.03.004]

9 **Shindoh J**, Truty MJ, Aloia TA, Curley SA, Zimmitti G, Huang SY, Mahvash A, Gupta S, Wallace MJ, Vauthey JN. Kinetic growth rate after portal vein embolization predicts posthepatectomy outcomes: toward zero liver-related mortality in patients with colorectal liver metastases and small future liver remnant. *J Am Coll Surg* 2013; **216**: 201-209 [PMID: 23219349 DOI: 10.1016/j.jamcollsurg.2012.10.018]

10 **Eguchi S**, Rozga J, Lebow LT, Chen SC, Wang CC, Rosenthal R, Fogli L, Hewitt WR, Middleton Y, Demetriou AA. Treatment of hypercholesterolemia in the Watanabe rabbit using allogeneic hepatocellular transplantation under a regeneration stimulus. *Transplantation* 1996; **62**: 588-593 [PMID: 8830820]

11 **Fogli L**, Morsiani E, Bertanti T, Eguchi S, Azzena G, Demetriou AA. Pancreatic beta-cell replication in streptozotocin-diabetic rats: the effect of liver compensatory growth on intraportally engrafted islets. *Pancreas* 1999; **19**: 304-309 [PMID: 10505762]

12 **Lainas P**, Boudechiche L, Osorio A, Coulomb A, Weber A, Pariente D, Franco D, Dagher I. Liver regeneration and recanalization time course following reversible portal vein embolization. *J Hepatol* 2008; **49**: 354-362 [PMID: 18387688 DOI: 10.1016/j.jhep.2008.01.034]

13 **Ichikawa T**, Taura N, Miyaaki H, Matsuzaki T, Ohtani M, Eguchi S, Takatsuki M, Soyama A, Hidaka M, Okudaira S, Usui T, Mori S, Kamihira S, Kanematsu T, Nakao K. Human T-cell leukemia virus type 1 infection worsens prognosis of hepatitis C virus-related living donor liver transplantation. *Transpl Int* 2012; **25**: 433-438 [PMID: 22417010 DOI: 10.1111/j.1432-2277.2012.01434.x]

14 **Kokudo N**, Tada K, Seki M, Ohta H, Azekura K, Ueno M, Ohta K, Yamaguchi T, Matsubara T, Takahashi T, Nakajima T, Muto T, Ikari T, Yanagisawa A, Kato Y. Proliferative activity of intrahepatic colorectal metastases after preoperative hemihepatic portal vein embolization. *Hepatology* 2001; **34**: 267-272 [PMID: 11481611]

15 **Aussilhou B**, Lesurtel M, Sauvanet A, Farges O, Dokmak S, Goasguen N, Sibert A, Vilgrain V, Belghiti J. Right portal vein ligation is as efficient as portal vein embolization to induce hypertrophy of the left liver remnant. *J Gastrointest Surg* 2008; **12**: 297-303 [PMID: 18060468]

16 **Ribero D**, Abdalla EK, Madoff DC, Donadon M, Loyer EM, Vauthey JN. Portal vein embolization before major hepatectomy and its effects on regeneration, resectability and outcome. *Br J Surg* 2007; **94**: 1386-1394 [PMID: 17583900]

17 **Lesurtel M**, Belghiti J. Temporary portal vein embolization as a starter of liver regeneration. *J Hepatol* 2008; **49**: 313-315

[PMID: 18644648 DOI: 10.1016/j.jhep.2008.06.004]
18 **Khuu DN**, Nyabi O, Maerckx C, Sokal E, Najimi M. Adult human liver mesenchymal stem/progenitor cells participate in mouse liver regeneration after hepatectomy. *Cell Transplant* 2013; **22**: 1369-1380 [PMID: 23211283]
19 **Ghodsizad A**, Fahy BN, Waclawczyk S, Liedtke S, Gonzalez Berjon JM, Barrios R, Mehrabi A, Karck M, Ruhparwar A, Kögler G. Portal application of human unrestricted somatic stem cells to support hepatic regeneration after portal embolization and tumor surgery. *ASAIO J* 2012; **58**: 255-261 [PMID: 22543756 DOI: 10.1097/MAT.0b013e31824cc922]
20 **am Esch JS**, Schmelzle M, Fürst G, Robson SC, Krieg A, Duhme C, Tustas RY, Alexander A, Klein HM, Topp SA, Bode JG, Häussinger D, Eisenberger CF, Knoefel WT. Infusion of CD133+ bone marrow-derived stem cells after selective portal vein embolization enhances functional hepatic reserves after extended right hepatectomy: a retrospective single-center study. *Ann Surg* 2012; **255**: 79-85 [PMID: 22156926 DOI: 10.1097/SLA.0b013e31823d7d08]
21 **Gock M**, Eipel C, Linnebacher M, Klar E, Vollmar B. Impact of portal branch ligation on tissue regeneration, microcirculatory response and microarchitecture in portal blood-deprived and undeprived liver tissue. *Microvasc Res* 2011; **81**: 274-280 [PMID: 21397614 DOI: 10.1016/j.mvr.2011.03.005]
22 **van den Esschert JW**, van Lienden KP, Alles LK, van Wijk AC, Heger M, Roelofs JJ, van Gulik TM. Liver regeneration after portal vein embolization using absorbable and permanent embolization materials in a rabbit model. *Ann Surg* 2012; **255**: 311-318 [PMID: 22241291 DOI: 10.1097/SLA.0b013e31823e7587]
23 **Liska V**, Slowik P, Eggenhofer E, Treska V, Renner P, Popp FC, Mirka H, Kobr J, Sykora R, Schlitt HJ, Holubec L, Chlumska A, Skalicky T, Matejovic M, Dahlke MH. Intraportal injection of porcine multipotent mesenchymal stromal cells augments liver regeneration after portal vein embolization. *In Vivo* 2009; **23**: 229-235 [PMID: 19414408]
24 **Ozkan F**, Peynircioglu B, Cil BE. Portal vein embolization and stem cell administration. *Radiology* 2008; **246**: 646; author reply 646-647 [PMID: 18227559 DOI: 10.1148/radiol.2462070523]
25 **Fürst G**, Schulte am Esch J, Poll LW, Hosch SB, Fritz LB, Klein M, Godehardt E, Krieg A, Wecker B, Stoldt V, Stockschläder M, Eisenberger CF, Mödder U, Knoefel WT. Portal vein embolization and autologous CD133+ bone marrow stem cells for liver regeneration: initial experience. *Radiology* 2007; **243**: 171-179 [PMID: 17312278]
26 **Dagher I**, Nguyen TH, Groyer-Picard MT, Lainas P, Mainot S, Guettier C, Pariente D, Franco D, Weber A. Efficient hepatocyte engraftment and long-term transgene expression after reversible portal embolization in nonhuman primates. *Hepatology* 2009; **49**: 950-959 [PMID: 19152424 DOI: 10.1002/hep.22739]

P- Reviewers Helling TS, Ikeda K, Mizuno S, Silva R
S- Editor Gou SX **L- Editor** Stewart GJ **E- Editor** Zhang DN

百世登

Baishideng®

Published by **Baishideng Publishing Group Co., Limited**
Flat C, 23/F., Lucky Plaza,
315-321 Lockhart Road, Wan Chai, Hong Kong, China
Fax: +852-65557188
Telephone: +852-31779906
E-mail: bpgoffice@wjgnet.com
http://www.wjgnet.com

ISSN 1007-9327

© 2013 Baishideng. All rights reserved.

Hepatol Int (2013) 7:655–661
DOI 10.1007/s12072-012-9379-y

ORIGINAL ARTICLE

The expression of transporter OATP2/OATP8 decreases in undetectable hepatocellular carcinoma by Gd-EOB-MRI in the explanted cirrhotic liver

Masaaki Hidaka · Mitsuhisa Takatsuki · Sadayuki Okudaira · Akihiko Soyama · Izumi Muraoka · Takayuki Tanaka · Izumi Yamaguchi · Takanobu Hara · Hisamitsu Miyaaki · Tatsuki Ichikawa · Tomayoshi Hayashi · Ichiro Sakamoto · Kazuhiko Nakao · Tamotsu Kuroki · Takashi Kanematsu · Susumu Eguchi

Received: 12 January 2012 / Accepted: 23 May 2012 / Published online: 24 June 2012
© Asian Pacific Association for the Study of the Liver 2012

Abstract
Purpose The aim of this study is to evaluate the detectability of hepatocellular carcinoma (HCC) in the explanted cirrhotic liver using gadoxetic acid-enhanced magnetic resonance imaging (Gd-EOB-MRI) and the degree of organic anion transporter OATP2/OATP8 (OATP1B1/1B3) HCC which could not be preoperatively detected by multi-detector computed tomography (MD-CT) and Gd-EOB-MRI.
Methods Eleven patients (HBV 3, HCV 7, nonBnonC 1) out of 145 recipients of liver transplantation were analyzed. The detectability by each imaging modality and the expression of OATP2/OATP8 of HCC were analyzed using the whole liver thin sliced histological and immunohistochemical examination retrospectively.
Results The imaging examination detected 17 lesions of HCC by MDCT and/or Gd-EOB-MRI. Only one lesion detected by Gd-EOB-MRI had well differentiated and minute (7 mm) HCC. However, the histological examination revealed newly 11 lesions and one false-positive lesion of HCC in the explanted livers. The median diameter of the preoperatively undetectable HCC by imaging was 8 mm (2–12). The histological characteristic of the preoperatively undetectable HCC was well differentiated HCC (10/11). The accuracy rate in MDCT and Gd-EOB-MRI was 53.6 % (15/28) and 57.1 % (16/28). The rate of positive predictive value in MDCT and Gd-EOB-MRI was 93.7 % (15/16) and 94.2 % (16/17), respectively. The expression of OATP2/OATP8 in the preoperatively undetectable HCC was negative in nine lesions, was weak positive in two lesions.
Conclusions The detectability of Gd-EOB-MRI is almost equal to MDCT in a cirrhotic liver. Small HCCs were difficult to detect even with Gd-EOB-MRI. The transporter of OATP2/OATP8 was less expressed in the preoperatively undetectable HCCs.

Keywords Hepatocellular carcinoma · EOB-MRI · OATP · Transporter

Abbreviations

HCC	Hepatocellular carcinoma
Gd-EOB-MRI	Gadoxetic acid-enhanced magnetic resonance imaging
MD-CT	Multi-detector computed tomography
OATP	Organic anion transporter
MELD	Model for end-stage liver disease
AFP	Alpha-fetoprotein
PIVKAII	Protein induced by Vitamin K absence or antagonists-II
RFA	Radio frequency ablation
TACE	Trans-arterial chemoembolization
MRP	Multidrug-resistant protein

M. Hidaka · M. Takatsuki · S. Okudaira · A. Soyama · I. Muraoka · T. Tanaka · I. Yamaguchi · T. Hara · T. Kuroki · T. Kanematsu · S. Eguchi (✉)
Department of Surgery, Nagasaki University Graduate School of Biomedical Sciences, 1-7-1 Sakamoto, Nagasaki 852-8501, Japan
e-mail: sueguchi@nagasaki-u.ac.jp

H. Miyaaki · T. Ichikawa · K. Nakao
Department of Gastroenterology and Hepatology, Nagasaki University Graduate School of Biomedical Sciences, Nagasaki, Japan

T. Hayashi
Department of Pathology, Nagasaki University Hospital, Nagasaki, Japan

I. Sakamoto
Department of Radiological Sciences, Nagasaki University Graduate School of Biomedical Sciences, Nagasaki, Japan

Introduction

Hepatocellular carcinoma (HCC) is the seventh most common cancer in patients with chronic liver disease particularly with hepatitis B and C virus-related hepatic dysfunction such as liver cirrhosis in the world [1]. Early and adequate diagnosis of HCC in the patient underlying liver dysfunction by optimal imaging modalities is likely to contribute to select the treatment and management for HCC and affect the mortality after various treatments which are the resection, liver transplantation, radio frequency ablation (RFA) and trans-arterial chemoembolization (TACE) [2–5]. A guideline from the American Association for the Study of Liver diseases has recommended that nodules with 1–2 cm in diameter in a cirrhotic liver should be investigated with two dynamic studies, including either computed tomography (CT) scan, contrast ultrasound or magnetic resonance imaging (MRI) [4, 6]. In recent years, liver specific agent has improved the detection of liver tumors. Gadoxetate-ethoxybenzyl-diethylenetriamine (Gd-EOB-DTPA; Primovist, Bayer Schering Pharma AG, Berlin, Germany) has been used as the liver specific contrast agent for detection of HCC [7]. This agent is initially taken up by hepatocytes and excreted to the biliary system. In a rodent study, the gadoxetic acid was uptaken by organic anion-transporting polypeptide (OATP) 2/8 (OATP1B1/1B3) and the excreted to the biliary canaliculi through the export transporter, multidrug-resistant protein (MRP) 2 [8, 9]. Several reports indicated that the expression of hepatocyte transporter especially OATP2/OATP8 in HCC correlated with the enhancement of Gd-EOB-MRI in the hepatocyte phase [10–12].

Compared with MD-CT, some investigators indicated that Gd-EOB-MRI had significantly higher accuracy and sensitivity in the detection of small HCC in patients with normal liver and liver cirrhosis [13–15].

However, we have reported that there are some HCCs in the explanted cirrhotic liver in the liver transplantation which could not be detected by even current modalities [16]. It is uncertain about the degree of the expression in an undetectable HCC by the advanced modalities including GD-EOB-MRI and the real detectability of HCC in the cirrhotic explanted liver.

This study aims to reveal the real detectability of MD-CT and Gd-EOB-MRI and the expression of hepatocyte transporter of HCC in the explanted cirrhotic liver which could not be detected preoperatively even by Gd-EOB-MRI.

Methods

Patients

We had 146 cases in liver transplantation (LT) in our university from 1997 to July 2011. Between 2008 and 2010, 11 patients (HBV 3, HCV 7, nonBnonC 1) out of 145 cases of LDLT were analyzed. From 2008, Gd-EOB-MRI had been used for the diagnosis of all patients with HCC before LT. MD-CT and Gd-EOB-MRI were done to evaluate the status of HCC. Our policy of the indication of LDLT for the patients with HCC sticks to the Milan Criteria: solitary tumor <5 cm, multiple tumor <3 nodules and 3 cm [17, 18]. In Table 1, the details of these patients were described as follows: Child-Pugh score 9 (median, 6–13), MELD score 11.5 (7–16), AFP 9.6 ng/ml (3.2–506), and PIVKA-II 38 mAU/ml (10–80).

Imaging and diagnostic methods

Multi-detector CT technique

Computed tomography was performed with a 64-MDCT scanner (Aquilion 64, Toshiba Medical Systems) with the following scanning parameters: rotation time, 0.5 s; beam collimation, 64 × 0.5 mm^2; section thickness and interval, 3 and 2.4 mm, respectively; field of view, 32 cm; 120 kV; tube current, 250–350 mAs. All helical scans were started from the top of the liver and proceeded in a cephalocaudal direction. In each patient, unenhanced and three-phase (arterial, portal, and delayed phase) contrast-enhanced helical scans of the whole liver were obtained. Patients were instructed to hold their breath during scanning. A dose of 110–135 ml of nonionic contrast material (iomeprol; Iomeron, Bracco) was injected into an antecubital vein at a rate of 4–5 ml/s. An automatic bolus tracking program (Real Prep, Toshiba Medical Systems) was used to time the start of acquisition after contrast injection.

MR imaging technique

Magnetic resonance imaging was performed with a 1.5T superconducting system (Signa, GE Medical Systems, Milwaukee, WI, USA), using a body-phased array multicoil for signal detection. Unenhanced sequences included breath-hold T2-weighted single-shot FSE sequences with and without fat saturation, and breath-hold T1-weighted GRE dual-echo "in and out of phase". Contrast-enhanced sequences were acquired after intravenous injection of Gd-EOB-DTPA at a dose of 0.1 ml/kg body weight at a speed

Table 1 Accuracy, sensitivity and positive predictive value of MD-CT, Gd-EOB-MRI

	MD-CT	Gd-EOB-MRI	*p* value
Accuracy	53.5 % (15/28)	57.1 % (16/28)	NS
Sensitivity	55.5 % (15/27)	59.2 % (16/27)	NS
Positive predictive rate	88.2 % (15/17)	94.1 % (16/17)	NS

of 1.5 ml/s, immediately followed by a 20-ml saline flush, using a dual power injector. Both dynamic and hepatobiliary-phase images were obtained using a fat-suppressed, 3D GRE sequence (liver acquisition with volume acceleration: LAVA, GE Medical Systems) before and after IV bolus administration of Gd-EOB-DTPA. Imaging delay-times were determined with an automatic bolus-tracking program (Smart Prep, GE Medical Systems) after contrast agent administration. Hepatic arterial phase images were obtained 10 s after the arrival of contrast medium in the proximal abdominal aorta, and portal venous and equilibrium phase images were obtained, respectively, 60 and 180 s after the beginning of the injection. Finally, hepatobiliary-phase imaging was obtained 20 min after the beginning of contrast-medium injection.

Diagnosis of HCC by imaging

Images were diagnosed by experienced radiologist before LT. Criteria for the diagnosis of HCC was shown as follows. HCC was diagnosed if two imaging characteristics were met: (1) the nodule was seen to clearly enhance during the hepatic arterial phase in MD-CT, Gd-EOB-MRI or (2) the nodule had washout during portal venous phase in MD-CT, and had hypo-intense to the surrounding liver during the hepatobiliary phase.

Histopathologic analysis

The detectability in each imaging modality was analyzed using the whole liver thin sliced histological examination [16]. Explanted livers were fixed in 10 % formalin for 48 h. The livers were then sectioned and serial sections were cut from paraffin blocks. Each section carefully was made from the paraffin-embedded blocks and stained with hematoxylin and eosin. Suspicious nodules by gross inspection were examined by an experienced pathologist (co-author S.O. T.H.). The pathological diagnoses and analyses were made according to the third edition of *The General Rules for the Clinical and Pathological Study of Primary Liver Cancer,* published by the Liver Cancer Study Group of Japan (LCSGJ) and Consensus for small hepatocellular carcinoma [19].

Immunohistochemical examination was performed as follows. Sections were deparafinized by ethanol concentrations and washed in tris–phosphate-buffered saline (TBS). Then, the sections in pH 6.0 citric acid buffer solution were treated with microwave at 125 °C for antigen retrieval for 10 min.

After washing, these were treated with 0.1 % H_2O_2 at room temperature for 10 min. The sections were reacted at room temperature for 60 min with primary monoclonal antibodies against OATP2/OATP8 (OATP1B1/1B3) (1:30) (Cat. No. 651140, Progen Biotechnik, Heidelberg. Germany). Secondary antibody (Envision^{TM}; DAKO, Chicago, USA) was used at room temperature for 30 min. The sections were stained with 3,3-diaminobenzidine tetrahydrochloride (DAB) for visualization. The sections were counterstained with Mayer's Hematoxylin.

Statistical analysis

The diagnostic accuracy, sensitivity, and positive predictive value of MD-CT and Gd-EOB-MRI in the diagnosis of HCC were evaluated of all lesions. The suspicious lesions were assessed and measured by a radiologist. The macroscopic lesions of HCC were assessed and measured by a pathologist in each section. In this retrospective analysis, the accuracy of diagnosis was calculated as the real number of HCCs in the whole explanted liver examination and number of true-negative lesions divided by the number of HCCs and false-positive, false-negative lesions and true-negative lesions [16]. Sensitivity was calculated as the number of true-positive lesions divided by the total number of HCCs. Positive predictive value was calculated as the number of HCCs divided by the number of HCCs and the number of false-positive lesions. A Chi-square test was used in the differences of accuracy, sensitivity and positive predictive value between MD-CT and Gd-EOB-MRI. Significance level was considered statistically significant when the p values were <0.05. Statistical analysis was done by SPSS Version 18.0.

Results

Accuracy, sensitivity and positive predictive value

Preoperative evaluation of HCC in the patients with LC detected 17 lesions in 11 patients by MD-CT and/or Gd-EOB-MRI, however, one nodule was only detected by Gd-EOB-MRI before LT. The histological whole-liver examination revealed newly 11 lesions of HCC and one false-positive lesion in the explanted livers. A total of HCC in the explanted liver was 28 nodules.

In comparison of the diagnostic accuracy, sensitivity and positive predictive value of HCC in MDCT and Gd-EOB-MRI, all parameters were greater with Gd-EOB-MRI than MDCT [accuracy Gd-EOB-MRI vs. MDCT: 57.1 % (16/28) vs. 53.5 % (15/28); sensitivity: 59.2 % (16/27) vs. 55.5 % (15/27); positive predictive value: 94.1 % (16/17) vs. 88.2 % (15/17)], respectively (Table 1). The HCC only detected by Gd-EOB-MRI was a hypervascular nodule at arterial phase, an iso-intense nodule during the hepatobiliary phase, and was 8 mm in a diameter and well differentiated tumor in the pathological findings.

Table 2 The characteristics of detectable and undetectable HCC in the explanted liver

	Detectable HCC ($n = 16$)	Undetectable HCC ($n = 11$)	p value
MD-CT			
Hypervascular	86.7 % (13/15)		
Wash out	33.3 % (5/15)		
Gd-EOB-MRI			
Hypervascular	81.3 % (13/16)		
Hypo-intense (hepatobiliary phase)	68.8 % (11/16)		
Diameter (cm)	1.85 (0.7–4.2)	0.8 (0.2–1.1)	<0.001
Differentiation			
Well	13	9	0.97
Moderate	3	2	

Pathological comparison of preoperatively detected and undetected HCC

A total of 17 lesions were detected by Gd-EOB-MRI and/or MDCT. Eleven hypervascular nodules and 8 hypovascular nodules were detected by MDCT. Thirteen hypervascular nodules and 11 hypo-intense nodules at the hapatocyte phase were detected by Gd-EOB-MRI.

The mean tumor diameter of preoperatively undetectable HCC was significantly smaller than that of detected HCC (undetectable HCC: median diameter 0.8 cm, range 0.2–1.1 cm vs. detectable HCC: 1.85 cm, range 0.7–4.2 cm; $p < 0.001$). However, the differentiation of these tumors was similar (undetectable HCC: 13 well, 3 moderate vs. detectable HCC: 9 well, 2 moderate; $p = 0.97$) (Table 2).

The expression of OATP2/OATP8 in the undetectable HCCs by Gd-EOB-MRI

The characteristics and expression of OATP2/OATP8 in the undetectable HCC by Gd-EOB-MRI was shown in the Table 2 and Figs. 2, 3. The no expression of OATP2/OATP8 in HCC and the expression of OATP2/OATP8 in liver parenchyma with liver cirrhosis are shown in Fig. 1. The negative and weak expression of OATP2/OATP8 in the undetectable HCC was shown in Figs. 2, 3. Nine lesions of the undetectable HCC had the negative of the expression of OATP2/OATP8, weak expression was shown in two lesions.

Discussion

Some reports indicated that the detectability of HCC was significantly higher in the Gd-EOB- MRI than MD-CT in the normal liver, and even though in cirrhotic liver [13–15]. The results of the present study revealed that there were HCCs in the cirrhotic liver which can not be detected preoperatively by even Gd-EOB-MRI, although the accuracy of Gd-EOB-MRI was superior to MD-CT. These data were based on the weakness of contrast in the hepatic phase by Gd-EOB-MRI as the uptake of the contrast agent in the cirrhotic liver was decreased [20, 21]. Usually the border between HCC lesion and normal liver was identified clearly in the hepatic phase, however, the image contrast in the cirrhotic liver was not clear in the border between the malignant lesion and the normal liver. Di Martino et al. [15] reported that the detectability of HCC <2 cm by Gd-EOB-MRI was significantly higher than MDCT. Mita et al. [22] indicated that there was no difference between Gd-EOB-MRI, Sonazoid contrast-enhanced ultrasonography and CT arterioportal angiography for diagnosing HCC in nodules smaller than 2 cm. Tajima et al. [21] reported that the degree of liver enhancement was significantly lower in the chronic liver dysfunction than the normal liver-function group. The cirrhotic liver has the potential of multi-centric carcinogenesis and the minute HCC which we had reported before [16]. The characteristic of undetectable HCC was minute nodule smaller than 1 cm (median diameter: 8 mm). The difficulty in the diagnosis of small HCCs might be associated that the border between small HCCs and cirrhotic liver was unclear

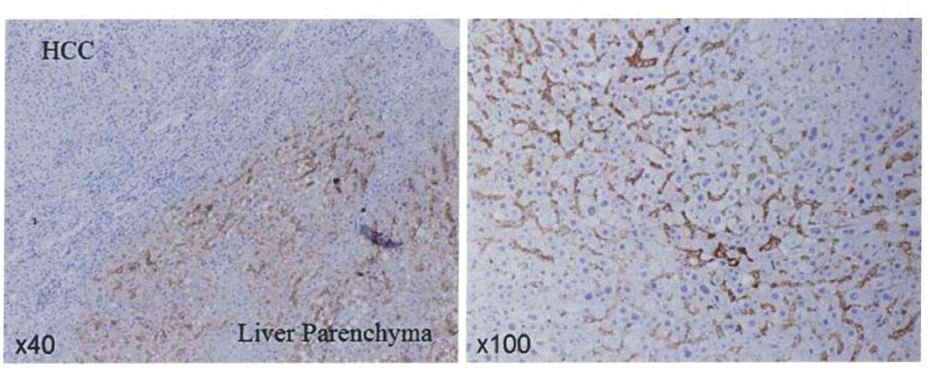

Fig. 1 The expression of OATP2/OATP8 in liver parenchyma and HCC

OATP2/OATP8 (liver parenchyma in LC)

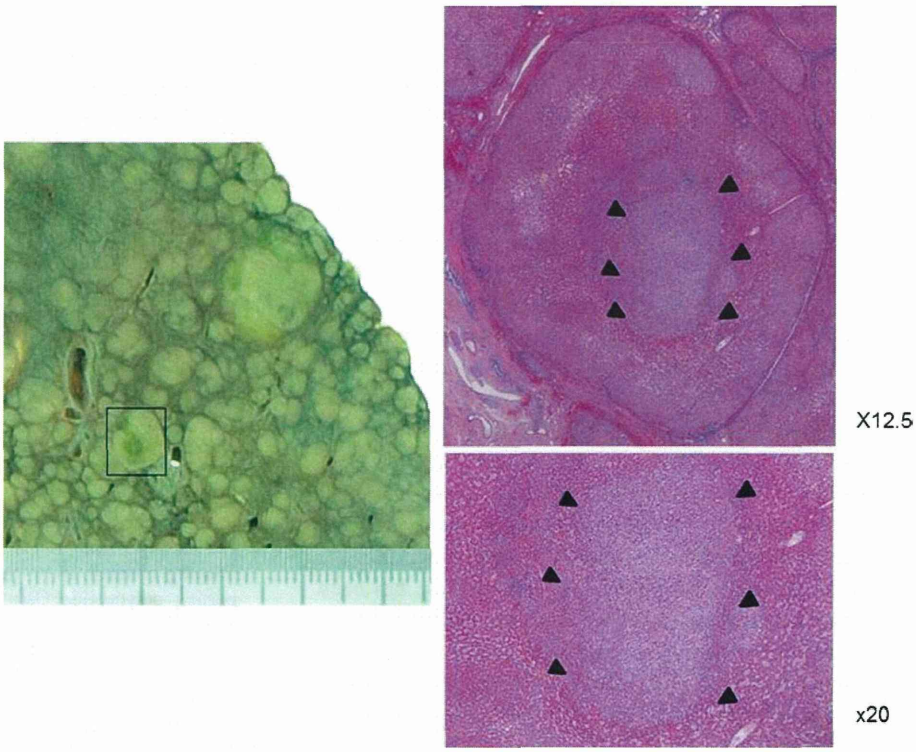

Fig. 2 An undetectable HCC by Gd-EOB-MRI, well differentiated, 8 mm in a dysplastic nodule

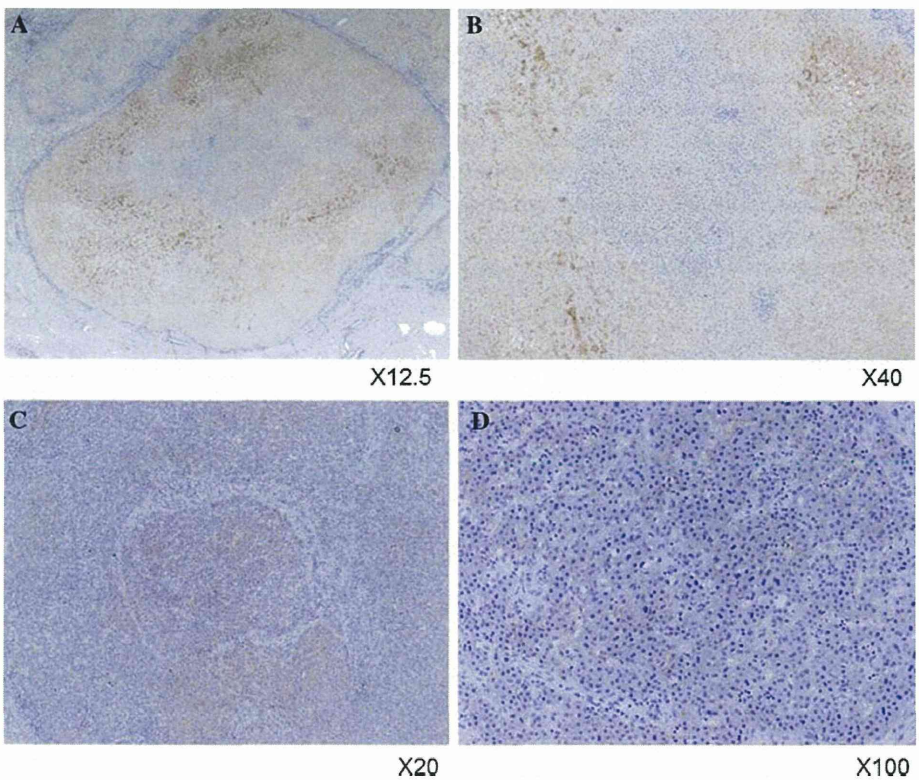

Fig. 3 **a**, **b** No expression of OATP. **c**, **d** Weak expression in undetectable HCC by Gd-EOB-MRI

in the hepatobiliary phase. Though the modalities of the image have progressed, it was difficult to detect the minute HCC in the cirrhotic liver by even Gd-EOB-MRI, because our patient had the end-staged liver disease with high Child-Pugh score and MELD score.

Recent studies investigated whether the transporter of Gd-EOB-MRI was expressed in the HCC with various types. There was some HCC which had high intensity of hepatocyte phase in Gd-EOB-MRI even with the expression of OATP transporter [10]. These lesions were so-called green hepatoma. These indicated the degree of contrast in the hepatic phase has been increased as the OATP1B3 has been more expressed in the HCC lesion. The present study revealed that the minute HCC in the explanted liver which has not been detected even by Gd-EOB-MRI had no and less expression of OATP2/OATP8. These findings might indicate the loss of membrane transporter in the normal hepatocyte during the process of the carcinogenesis of HCC. The transporter of the membrane of hepatocyte in the dysplastic nodule has been maintained, thereafter, has been lost the function of the membrane during the carcinogenesis. However, in some cases, the expression of OATP2/OATP8 in the moderate HCC has acquired the expression of transporter in such as the green hepatoma. This suggests that there might be an association of the transporter with the multi resistance drug protein, which excretes part of the Gd-EOB-MRI into the bile duct and bile canal. As the tumor has increased gradually to the moderate differentiation, the failure and compression of the bile duct in HCC has occured. The early HCC may have lost the expression of the OATP2/OATP8 function on the membrane of carcinogenic hepatocyte at first with the multi step carcinogenesis. Kitao et al. [23] reported that the expression of OATP8 significantly decreases during multistep hepatocarcinogenesis. The less expression of OATP2/OATP8 has the potential biomarker of early HCC such as Glypican 3 and heat shock protein (HSP) 70 [24, 25].

Conclusion

The detectability of HCC by Gd-EOB-MRI is almost equal to MDCT in a cirrhotic liver. Small HCCs were difficult to detect even with Gd-EOB-MRI. The transporter of OATP2/OATP8 was less expressed in the preoperatively undetectable HCCs.

Conflict of interest No conflict of interest.

References

1. Yang JD, Robert LR. Hepatocellular carcinoma: a global view. Nat Rev Gastroenterol Hepatol 2010;7:448–458
2. Bruix J, Sherman M. Management of hepatocellular carcinoma: an update: Hepatology 2011;53:1020–1022
3. Bruix J, Sherman M. Management of hepatocellular carcinoma. Hepatology 2005;42:1208–1236
4. Arii S, Sata M, Sakamoto M, Shimada M, Kumada T, Shiina S, Kumada T, Shiina S, Yamashita T, Kokudo N, Tanaka M, Takayama T, Kudo M. Management of hepatocellular carcinoma: report of consensus meeting in the 45th annual meeting of the Japan Society of Hepatology (2009). Hepatol Res 2010;40: 667–685
5. Minami Y, Kudo M. Radiofrequency ablation of hepatocellular carcinoma: current status. World J Radiol 2010;28:417–424
6. Forner A, Vilana R, Ayuso C, Bianchi L, Solé M, Ayuso JR, Boix L, Sala M, Varela M, Llovet JM, Brú C, Bruix J. Diagnosis of hepatic nodules 20 mm or smaller in cirrhosis: prospective validation of the noninvasive diagnostic criteria for hepatocellular carcinoma. Hepatology 2008;47:97–104
7. Kim MJ. Current limitations and potential breakthroughs for the early diagnosis of hepatocellular carcinoma. Gut Liver 2011;5: 15–21
8. van Montfoort JE, Stieger B, Meijer DK, Weinmann HJ, Meier PJ, Fattinger KE. Hepatic uptake of the magnetic resonance imaging contrast agent gadoxetate by the organic anion transporting polypeptide Oatp1. J Pharmacol Exp Ther 1999;290: 153–157
9. Lorusso V, Pascolo L, Fernetti C, Visigalli M, Anelli P, Tiribelli C. In vitro and in vivo hepatic transport of the magnetic resonance imaging contrast agent B22956/1: role of MRP proteins. Biochem Biophys Res Commun 2002;293:100–105
10. Narita M, Hatano E, Arizono S, Miyagawa-Hayashino A, Isoda H, Kitamura K, Taura K, Yasuchika K, Nitta T, Ikai I, Uemoto S. Expression of OATP1B3 determines uptake of Gd-EOB-DTPA in hepatocellular carcinoma. J Gastroenterol 2009;44:793–798
11. Tsuboyama T, Onishi H, Kim T, Akita H, Hori M, Tatsumi M, Nakamoto A, Nagano H, Matsuura N, Wakasa K, Tomoda K. Hepatocellular carcinoma: hepatocyte-selective enhancement at gadoxetic acid-enhanced MR imaging: correlation with expression of sinusoidal and canalicular transporters and bile accumulation. Radiology 2010;255:824–833
12. Kitao A, Zen Y, Matsui O, Gabata T, Kobayashi S, Koda W, Kozaka K, Yoneda N, Yamashita T, Kaneko S, Nakanuma Y. Hepatocellular carcinoma: signal intensity at gadoxetic acid-enhanced MR imaging: correlation with molecular transporters and histopathologic features. Radiology 2010;256:817–826
13. Ichikawa T, Saito K, Yoshioka N, Tanimoto A, Gokan T, Takehara Y, Kamura T, Gabata T, Murakami T, Ito K, Hirohashi S, Nishie A, Saito Y, Onaya H, Kuwatsuru R, Morimoto A, Ueda K, Kurauchi M, Breuer J. Detection and characterization of focal liver lesions: a Japanese phase III, multicenter comparison between gadoxetic acid disodium-enhanced magnetic resonance imaging and contrast-enhanced computed tomography predominantly in patients with hepatocellular carcinoma and chronic liver disease. Invest Radiol 2010;45:133–141
14. Kim SH, Kim SH, Lee J, Kim MJ, Jeon YH, Park Y, Choi D, Lee WJ, Lim HK. Gadoxetic acid-enhanced MRI versus triple-phase MDCT for the preoperative detection of hepatocellular carcinoma. AJR Am J Roentgenol 2009;192:1675–1681
15. Di Martino M, Marin D, Guerrisi A, Baski M, Galati F, Rossi M, Brozzetti S, Masciangelo R, Passariello R, Catalano C. Intraindividual comparison of gadoxetate disodium-enhanced MR imaging and 64-section multidetector CT in the detection of hepatocellular carcinoma in patients with cirrhosis. Radiology 2010;256:806–816
16. Hidaka M, Eguchi S, Okudaira S, Takatsuki M, Tokai H, Soyama A, Nagayoshi S, Mochizuki S, Hamasaki K, Tajima Y, Kanematsu T. Multicentric occurrence and spread of hepatocellular

carcinoma in whole explanted end-stage liver. Hepatol Res 2009; 39:143–148
17. Mazzaferro V, Regalia E, Doci R, Andreola S, Pulvirenti A, Bozzetti F, Montalto F, Ammatuna M, Morabito A, Gennari L. Liver transplantation for the treatment of small hepatocellular carcinomas in patients with cirrhosis. N Engl J Med 1996;334: 693–699
18. Eguchi S, Takatsuki M, Hidaka M, Tajima Y, Kanematsu T. Evolution of living donor liver transplantation over 10 years: experience of a single center. Surg Today 2008;38:795–800
19. International Consensus Group for Hepatocellular Neoplasia. Pathologic diagnosis of early hepatocellular carcinoma: a report of the international consensus group for hepatocellular neoplasia. Hepatology 2009;49:658–664
20. Motosugi U, Ichikawa T, Sou H, Sano K, Tominaga L, Kitamura T, Araki T. Liver parenchymal enhancement of hepatocyte-phase images in Gd-EOB-DTPA-enhanced MR imaging: which biological markers of the liver function affect the enhancement? J Magn Reson Imaging 2009;30:1042–1046
21. Tajima T, Takao H, Akai H, Kiryu S, Imamura H, Watanabe Y, Shibahara J, Kokudo N, Akahane M, Ohtomo K. Relationship between liver function and liver signal intensity in hepatobiliary phase of gadolinium ethoxybenzyl diethylenetriamine pentaacetic acid-enhanced magnetic resonance imaging. J Comput Assist Tomogr 2010;34:362–366
22. Mita K, Kim SR, Kudo M, Imoto S, Nakajima T, Ando K, Fukuda K, Matsuoka T, Maekawa Y, Hayashi Y. Diagnostic sensitivity of imaging modalities for hepatocellular carcinoma smaller than 2 cm. World J Gastroenterol 2010;16:4187–4192
23. Kitao A, Matsui O, Yoneda N, Kozaka K, Shinmura R, Koda W, Kobayashi S, Gabata T, Zen Y, Yamashita T, Kaneko S, Nakanuma Y. The uptake transporter OATP8 expression decreases during multistep hepatocarcinogenesis: correlation with gadoxetic acid enhanced MR imaging. Eur Radiol 2011;21:2056–2066
24. Ma M, Sakamoto M, Yamazaki K, Ohta T, Ohki M, Asaka M, Hirohashi S. Expression profiling in multistage hepatocarcinogenesis: identification of HSP70 as a molecular marker of early hepatocellular carcinoma. Hepatology 2003;37:198–207
25. Stefaniuk P, Cianciara J, Wiercinska-Drapalo A. Present and future possibilities for early diagnosis of hepatocellular carcinoma. World J Gastroenterol 2010;16:418–424